Journal of Catalysis **183,** 169–181 (1999)
Article ID jcat.1999.2391, available online at http://www.idealibrary.com on IDEAL®

Identification of Copper Species Present in Cu-ZSM-5 Catalysts for NO_x Reduction

Graeme J. Millar,[1] Arran Canning, Graham Rose, Barry Wood, Lisa Trewartha, and Ian D. R. Mackinnon*

*Department of Chemistry and *The Centre for Microscopy and Microanalysis, The University of Queensland, St. Lucia, Brisbane, Queensland 4072, Australia*

Received March 9, 1998; revised December 10, 1998; accepted December 12, 1998

The structure of Cu-ZSM-5 catalysts that show activity for direct NO decomposition and selective catalytic reduction of NO_x by hydrocarbons has been investigated by a multitude of modern surface analysis and spectroscopy techniques including X-ray photoelectron spectroscopy, thermogravimetric analysis, and *in situ* Fourier transform infrared spectroscopy. A series of four catalysts were prepared by exchange of Na-ZSM-5 with dilute copper acetate, and the copper loading was controlled by variation of the solution pH. Underexchanged catalysts contained isolated $Cu^{2+}OH^{-}(H_2O)$ species and as the copper loading was increased Cu^{2+} ions incorporated into the zeolite lattice appeared. The sites at which the latter two copper species were located were fundamentally different. The $Cu^{2+}OH^{-}(H_2O)$ moieties were bound to two lattice oxygen ions and associated with one aluminum framework species. In contrast, the Cu^{2+} ions were probably bound to four lattice oxygen ions and associated with two framework aluminum ions. Once the Cu-ZSM-5 samples attained high levels of exchange, the development of $[Cu(\mu\text{-}OH)_2Cu]^{2+}_n OH^{-}(H_2O)$ species along with a small concentration of $Cu(OH)_2$ was observed. On activation in helium to 500°C the $Cu^{2+}OH^{-}(H_2O)$ species transformed into $Cu^{2+}O^{-}$ and Cu^{+} moieties, whereas the Cu^{2+} ions were apparently unaffected by this treatment (apart from the loss of ligated water molecules). Calcination of the precursors resulted in the formation of $Cu^{2+}O_2^{-}$ and a one-dimensional CuO species. Temperature-programmed desorption studies revealed that oxygen was removed from the latter two species at 407 and 575°C, respectively.

INTRODUCTION

Nitrogen oxides (NO_x) are by-products of high-temperature combustion processes and are a significant factor in the production of "acid rain," a ubiquitous product in most industrialized countries. Nitrogen oxides are produced mainly from the combustion of fossil fuels (e.g., in coal-fired power stations and motor vehicles) and are linked to a series of health problems including bronchitis, pneumonia, susceptibility to viral infection, and alterations of the immune system. The use of "three-way" catalysts based on platinum, rhodium, and ceria, in automotive vehicles operating at the stoichiometric air/fuel ratio of 14.7 : 1, is well established (1). However, there is a continuing desire to further improve their performance and durability in the light of ever-stricter environmental legislation. Furthermore, it is evident that future trends will be toward the use of "lean-burn" engines that provide the dual advantages of increased fuel efficiency and decreased pollutant emissions. Unfortunately, although CO and hydrocarbons are readily oxidized under lean conditions the "three-way" catalyst is relatively inefficient at reducing NO_x emissions. Consequently, the search for a NO_x reduction catalyst has been of considerable interest (2–5). Copper-exchanged ZSM-5 has been the subject of substantial research primarily due to the pioneering studies of Iwamoto and co-workers (6) which indicated that NO could be directly decomposed into its constituent elements at relatively low temperatures. This field of study was enhanced by the discovery that an entire series of metal-exchanged zeolites showed good activity for the selective reduction of NO_x by hydrocarbons in the presence of excess oxygen. Cu-ZSM-5 does not appear to possess either the necessary high activity or stability under actual exhaust conditions (7). Nevertheless, it is important to determine the mechanism by which the catalyst operates to provide a logical approach to future NO_x reduction catalyst development.

Several excellent reviews have been published (2–5, 8) and it is apparent that no general consensus of opinion exists with respect to the nature of the active site involved or indeed the reaction mechanism occurring. The main points of dispute can be summarized as follows: (1) Considerable evidence has been provided to indicate that Cu^{+} species participate in the reaction (9, 10). A detailed redox mechanism has been outlined by Hall and co-workers (11, 12). In contrast, Shelef (2) has postulated that the reaction proceeds entirely on Cu^{2+} species involving the *gem*-dinitrosyl species. (2) The NO decomposition reaction is promoted on "overexchanged" Cu- ZSM-5 catalysts and this behavior may correlate with the availability of "extra-lattice-oxygen

[1] To whom correspondence should be addressed. Fax: (61) 7 3365 4299. E-mail: millar@chemistry.uq.oz.au.

0021-9517/99 $30.00

(ELO) species" (13). The identity of the ELO is not clear as Sachtler and co-workers (14, 15) have proposed that it is of the form "Cu^{2+}–O^{2-}–Cu^{2+}," whereas Bell and co-workers (16) have suggested that the ELO is associated with isolated Cu^{2+} sites and is of the structure $Cu^{2+}O^-$ or $Cu^{2+}O_2^-$. (3) The mechanism for coupling of nitrogen species to form product N_2 is a topic of controversy. Aylor *et al.* (17) considered that reaction between adjacent pairs of nitrosyl species on Cu^+ sites initially occurred to form N_2O which subsequently decomposed on Cu^+ sites to form N_2. In contrast, Chang and McCarty (18) demonstrated, using isotopic studies, that adsorbed NO_2 species were important during NO decomposition. Centi and Perathoner (8) have amplified the discussion by eluding to the possibility of multiple mechanistic pathways, the dominant mechanism depending on the reaction environment. Under transient conditions a reaction can transpire between two adsorbed nitrosyl species or perhaps dissociative chemisorption of NO could occur. Alternatively, under stationary conditions it is hypothesized that reaction pairing is achieved by coordination of a nitrosyl and a nitro species on a copper site and consequent rearrangement to form an N_2O_3 intermediate.

Thus, it is apparent that substantial debate still surrounds the mechanism by which Cu-ZSM-5 catalysts operate in NO_x reduction. Fundamental to the resolution of the controversy surrounding the mode by which Cu-ZSM-5 operates is the characterization of the copper species that are present. Therefore, this study attempts to enlighten this debate by using a multitude of modern surface analysis and spectroscopic methods to determine the copper species present in a range of catalysts of varying copper content and to subsequently relate the adsorption properties to the identified catalytic sites.

EXPERIMENTAL

A range of copper-exchanged ZSM-5 samples were prepared similarly to the procedures outlined by Flytzani-Stephanopoulos and co-workers (19). Briefly, a 0.007 M aqueous solution of cupric acetate (BDH, AnalaR grade) was made and the pH then adjusted by the addition of aqueous ammonia to give a final pH of either 5.5, 6.0, or 6.5. Subsequently, Na-ZSM-5 (Uetikon, ZEOCAT PZ-2/25) with a SiO_2/Al_2O_3 ratio of 24 and a BET surface area of 400 $m^2\,g^{-1}$ was added in sufficient quantities such that all the Na^+ ions were replaced by half the number of Cu^{2+} species. The solution was stirred for 19 h at ambient temperature and then filtered. The resultant sample was then extensively washed with deionized water and dried overnight at 100°C. This exchange procedure was twice further performed on each sample. An "underexchanged" sample was also prepared by executing one exchange process at a pH of 5.7. ICP analysis indicated that the catalysts were exchanged to the extent of 52% (pH 5.7 "underexchanged," Cu-ZSM-5-52), 54% (pH 5.5, Cu-ZSM-5-54), 102% (pH 6.0, Cu-ZSM-5-102), and 195% (pH 6.5, Cu-ZSM-5-195).

X-ray photoelectron spectroscopy (XPS) analysis was performed using a Physical Electronics Industries PHI Model 560 surface analysis system. This system employs a double-pass CMA (20-270AR) and a perpendicularly mounted dual (Mg/Al) X-ray source. A single Mg$K\alpha$ X-ray source was operated at 400 W and 15 kV. For the heating experiments pressed disks were mounted onto a PHI Model 02-121A high-temperature probe and the sample temperature was regulated by means of a Eurotherm digital temperature controller. Atomic concentrations were quantified using peak areas from 50-eV multiplex spectra (acquisition time, 5 min) and experimentally derived elemental sensitivity factors. High-resolution spectra of C 1*s*, Si 2*p*, and Cu 2*p* regions were obtained using a pass energy of 25 eV and 0.1-eV steps for 10 min. Sample charging was referenced to the Si 2*p* photoelectron peak of binding energy 102.9 eV. The short acquisition times were chosen so as to minimize reduction of Cu^{2+} species to Cu^+ ions by the X-ray flux as reported by several authors (20, 21). Careful examination of this effect was made and it was concluded that the conditions employed in this study did not lead to any detectable reduction of Cu^{2+} species at ambient temperature.

Thermogravimetric analysis (TGA) was performed using a Perkin–Elmer TGA 7 instrument with a TAC 7/DX thermal analysis controller in an atmosphere of purified nitrogen. Samples were heated linearly at 20°C/min to a temperature of 800°C.

Fourier transform infrared (FTIR) spectroscopic measurements were attained using a Perkin–Elmer 2000 FTIR spectrometer equipped with an MCT detector. Samples for *in situ* FTIR were pressed into a tungsten mesh grid which was then located in a transmission cell of the type described in detail by Yates and co-workers (22). All spectra were recorded in the region 4000–1000 cm^{-1}. For the region 1300–1000 cm^{-1} Si–O vibrational bands are too intense to show any adsorbing species, and at <1000 cm^{-1} CaF_2 windows located in the *in situ* cell restricted the transmission. For 4000–2800 cm^{-1} any adsorbing species were too weak to be noticed. Typically, a catalyst was initially activated by heating it in a flow of ultrahigh-purity helium (50 ml/min) to 500°C. The sample was then either allowed to remain at 500°C for 60 min in helium (autoreduced sample) or contacted with a 1% CO/He or 10% H_2/He mixture at 500°C (reduced samples) (designated "CO" or "auto" or "H_2," e.g., reduction of Cu-ZSM-5-195 with CO would be represented by Cu-ZSM-5-195-CO). After cooling the sample to ambient temperature in helium, a background spectrum of the pretreated catalyst was recorded at a resolution of 4 cm^{-1} averaged over 64 scans. Spectra were then taken following addition of the appropriate adsorbate and ratioed against the background spectrum. Carbon monoxide (1%

CO/He) was of ultrahigh-purity grade as supplied by BOC and was used without further purification.

Temperature-programmed desorption (TPD) experiments were achieved by use of a modified microreactor. Typically, 50 mg of catalyst was placed in a stainless-steel or quartz reactor tube of 4-mm internal diameter which was inserted into an electrically heated furnace. A thermocouple was embedded in the center of the catalyst plug and the temperature monitored with a Eurotherm 904 temperature programmable controller. Ultrahigh-purity gases were then regulated by a series of MKS mass flow controllers interfaced to an MKS 647B multigas digital control unit. Typically, adsorbing gases were introduced to the sample at 100 ml/min at 25°C for 30 min. During the desorption of the adsorbed species the helium was flowing at 50 ml/min. The effluent from the reactor was continuously monitored with a Balzers Thermocube quadrupole mass spectrometer operating in multiple ion detection mode and using Quadstar 421 software.

RESULTS

X-Ray Photoelectron Spectroscopy

Precursors

XPS was used to characterize the species present in the fresh copper-exchanged zeolite catalysts. The XPS region studied for copper was between 950 and 970 eV relative to Cu 2*p*, in particular the $2p_{1/2}$ and $2p_{3/2}$ levels. Figure 1 illustrates the Cu 2*p* spectra obtained for the series of copper-exchanged ZSM-5 samples of interest (all intensities were normalized against the Si 2*p* peak for ZSM-5). As a general observation the intensity of the peaks due to copper species exhibited a dramatic increase which correlated with the elevation of the solution pH during catalyst preparation. This result is in harmony with the study of Zhang *et al.* (19) as they also reported that Cu-ZSM-5 catalysts gradually attained greater exchange levels as the pH was raised from 4.5 to 7. Additionally, the presence of a shakeup feature at ca. 944 eV characteristic of Cu(II) species was noted primarily in the spectra for the highly exchanged catalysts (Figs. 1c and 1d). More detailed analysis of the XPS profiles was achieved by curve-fitting the $2p_{3/2}$ peak to determine the subbands present. The main peaks are summarized in Table 1 to aid in interpretation. The underexchanged sample (Fig. 2A) exhibited a distinct subband at 933.7 eV which was accompanied by a minor feature at ca. 936.2 eV, with evidence for a shakeup satellite at ca. 942.2 eV also apparent. Haack and Shelef (20) observed a similar band at 933.5 eV which was accompanied by a shakeup feature at ca. 942.5 eV (the latter authors did not deconvolute the satellite region although inspection of their data allowed a reasonable estimate of the subband position to be made). The only attempt at an assignment for this copper species was to mention a correspondence with the binding energy for CuO. More detailed information can be gleaned from the study of Grunert *et al.* (21) who have reported that copper species at our reported binding energy of 933.5 eV may be of the type Cu^{+}. However, it may be the case that this species is actually in the II oxidation state since a satellite feature accompanies the peak at 933.5 eV (Fig. 2A). Consequently, it is possible that the species of interest may have an overall charge of "1+" but still contain a copper(II) ion (as discussed below).

As the copper loading increased the subband at ca. 936.8 became more pronounced and concomitantly the shakeup feature at ca. 944.0 eV intensified (Fig. 2B). Deconvolution of the satellite structure suggested that two peaks were present at 945.5 and 943.0 eV (Fig. 2B). Haack and Shelef (20) noted the appearance of a core peak at 936.5 eV accompanied by a satellite at ca. 944.5 eV, and these were assigned to the presence of Cu^{2+} ions incorporated into the zeolite lattice. Significantly, as the copper exchange level was further enhanced an extra peak developed at ca. 935.0 eV which was also associated with the appearance of a third feature in the shakeup region at ca. 943.3 eV (Fig. 2C).

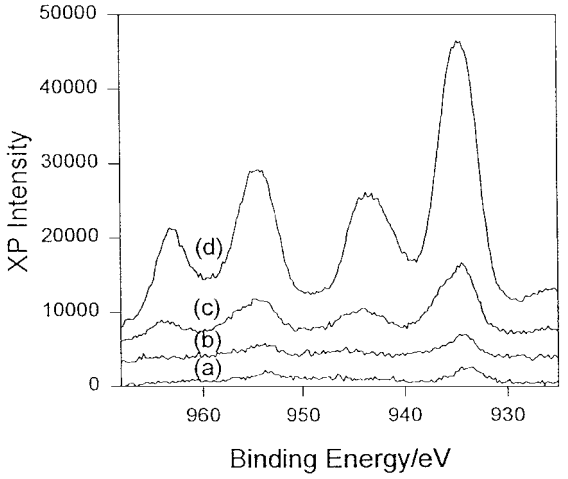

FIG. 1. X-ray photoelectron spectra of Cu $2p_{1/2}$ and Cu $2p_{3/2}$ levels for the precursors (a) Cu-ZSM-5-52, (b) Cu-ZSM-5-54, (c) Cu-ZSM-5-102, and (d) Cu-ZSM-5-195.

TABLE 1

Main XPS Subbands Calculated for Cu $2p_{1/2}$ Region for Uncalcined Catalysts

	Species I (eV)	Species II (eV)	Species III (eV)
Cu-ZSM-5-52	933.7		936.2
Cu-ZSM-5-54	934.2		936.8
Cu-ZSM-5-102	934.0	935.0	936.8
Cu-ZSM-5-195	933.7	935.0	936.5

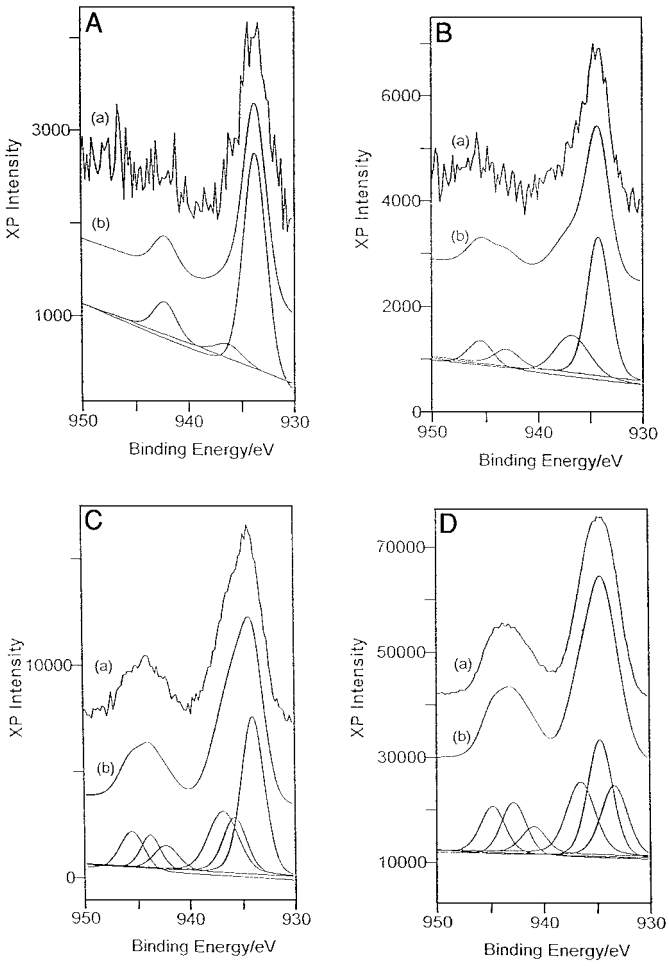

FIG. 2. XPS subband analysis of Cu $2p_{3/2}$ region for (A) Cu-ZSM-5-52, (B) Cu-ZSM-5-54, (C) Cu-ZSM-5-102, and (D) Cu-ZSM-5-195, where (a) is the raw spectrum and (b) is the calculated fit in each case. The remaining peaks are the subbands.

Indeed, for the catalyst of highest copper loading the subband at ca. 935.0 eV became the most abundant species and this observation is in agreement with the XPS data of Grünert *et al.* (21) for copper species in fresh Cu-ZSM-5 catalysts. To clarify the situation a graph relating the intensity of each subband in the core peak to the sample studied (and naturally the amount of copper present) was compiled (Fig. 3). It can be deduced from Fig. 3 that copper species represented by the subband at 933.7 eV were consistently present in all samples whereas the species responsible for the subbands at 935.0 and 936.8 eV displayed a dramatic increase in magnitude when the catalyst became overexchanged with copper species. From the position of the subband at ca. 935.0 eV it could be inferred that this peak corresponds to a species resembling $Cu(OH)_2$ (23). Support for this latter assignment is provided by examination of the magnitude of the splitting between the satellite peak and the core line (termed the satellite splitting energy, $\Delta\varepsilon$). The average value of ca. 8.00 eV is in reasonable agreement with the value quoted by Frost (24) of 7.6 eV for pure $Cu(OH)_2$. The possibility of $Cu(OH)_2$ deposition in zeolite pores at high pH values has previously been mentioned by Zhang *et al.* (19). Alternatively, more complex species of the type "$Cu(OH)_2CuOH$" anchored to the zeolite lattice as proposed by Kharas *et al.* (5) could also provide an explanation for the observed XPS peak at 935.0 eV and explain the discrepancy in the value of $\Delta\varepsilon$ relative to $Cu(OH)_2$.

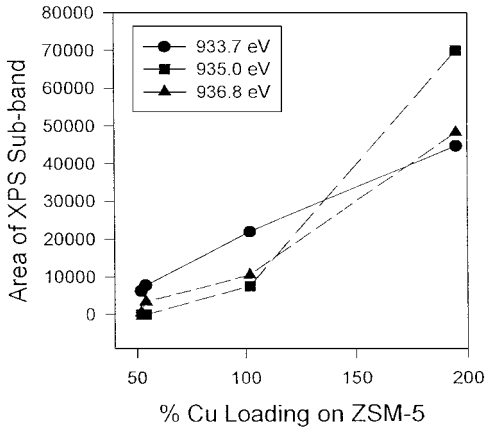

FIG. 3. Relationship between XPS subband area and the level of copper exchange for Cu-ZSM-5 after exchange.

Calcined Samples

The catalyst precursors were calcined in air for 2 h at 500°C and then characterized by XPS in the same manner as before (Fig. 4). The spectra of the calcined catalysts reflected those of the precursor samples in that the intensity of the copper peaks increased as the sample pH changed from 5.5 to 6.5 (cf. Figs. 1 and 4). However, it was apparent

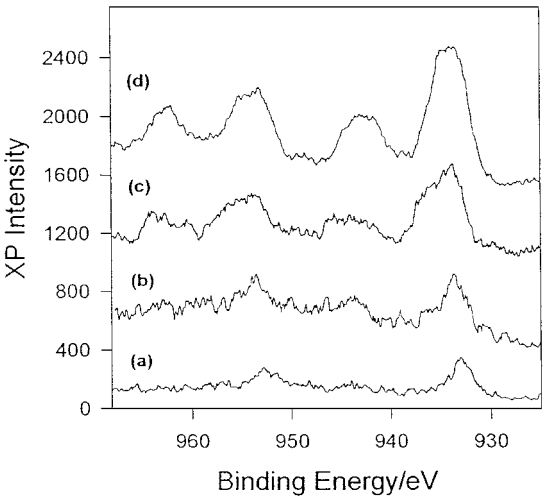

FIG. 4. X-ray photoelectron spectra of Cu $2p_{1/2}$ and Cu $2p_{3/2}$ for the calcined samples (a) Cu-ZSM-5- 52, (b) Cu-ZSM-5-54, (c) Cu-ZSM-5-102, and (d) Cu-ZSM-5-195.

that the difference in magnitude of the copper species detected between the various catalysts was not as great as in the precursor case. This behavior indicated that substantial migration of species deposited on the external zeolite surface to the inner channel structure may have been induced by the calcination procedure. This result has also been reported by Grünert *et al.* (21) who noted that dispersion of copper species occurred during catalyst pretreatment. Closer inspection of the copper $2p_{3/2}$ profile and the corresponding shakeup feature revealed more subtle differences. The underexchanged sample contained subbands at 944.0, 942.7, 934.2, and 932.7 eV. Haack and Shelef (20) reported that CuO species on ZSM-5 are represented by a peak at 933.5 eV and an associated shakeup at 943.5 eV which can be correlated with the peaks at 944.0 and 934.2 eV. The main peak at 932.7 eV and the associated shakeup peak at 942.7 eV probably indicated the presence of $Cu^{2+}O^{-}$ and $Cu^{2+}O_2^{-}$ species as suggested by Larsen *et al.* (16). The profile for calcined Cu-ZSM-5-54 consisted of additional subbands at 945.2 and 935.8 eV and notably the concentration of CuO species was enhanced in this catalyst. Significantly, the intensities of the subbands at 945.4 and 936.3 eV were substantially increased relative to those for CuO and the copper species represented by subbands at 942.2 and 932.9 eV when a catalyst prepared at pH 6.0 was calcined. For the calcined Cu-ZSM-5-195 sample the profile became dominated by features typical of CuO, and this trend was better revealed by inspection of the relevant graph of subband intensity versus the nature of Cu-ZSM-5 zeolite (Fig. 5). The subbands at 935.8 and 934.1 eV clearly increased at the greatest rate as the copper loading was increased. This behavior suggested that copper hydroxyl species represented by the subband at 935.0 eV on the fresh catalyst gave rise to CuO species (subband at 934.1 eV) after calcination. Furthermore, the copper species characterized by the subband at 936.8 eV in the fresh sample were most probably

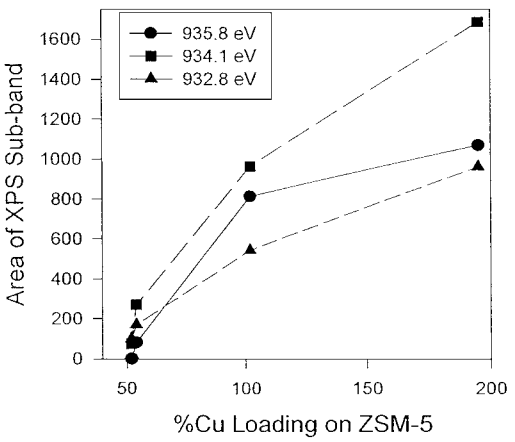

FIG. 5. Relationship between XPS subband area and the level of copper exchange for Cu-ZSM-5 after calcination.

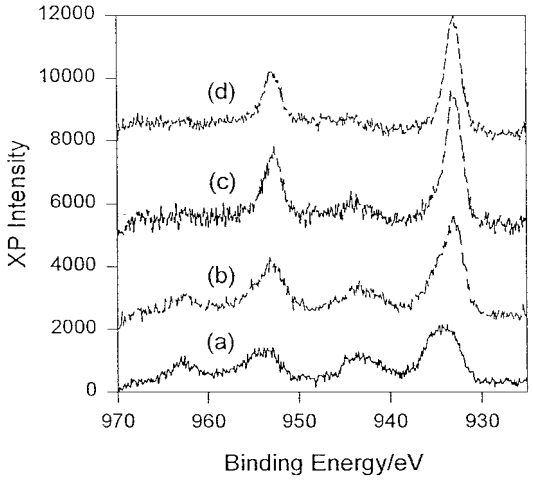

FIG. 6. *In situ* X-ray photoelectron spectra illustrating autodecomposition of Cu-ZSM-5-195 at (a) 20, (b) 200, (c) 460, and (d) 500°C.

transformed to structures represented by the subband at 935.8 eV in the calcined catalyst.

Transformations during Activation Procedure

Autodecomposition. It has often been reported that reduction of Cu^{2+} species to Cu^{+} ions occurs during heating of a Cu-ZSM-5 sample to 500°C (14, 16). An interesting way in which to examine this proposed transition is to use *in situ* XPS. Therefore, a high copper-exchanged ZSM-5 sample (Cu-ZSM-5-195) was mounted on the *in situ* probe in the XPS chamber and gradually heated to 500°C. The resultant *in situ* XPS profiles are displayed in Fig. 6. Heating the catalyst to 200°C (Fig. 6b) induced several spectral changes including a reduction in the intensity of the shakeup satellites and modification of the Cu 2*p* peaks to produce distinctly asymmetric bands. Curve-fitting of the Cu $2p_{3/2}$ peak facilitated the more detailed interpretation of these phenomena. Four subbands were identified at 936.7, 935.0, 933.3, and 932.6 eV and these were accompanied by the presence of three subbands at 944.9, 943.5, and 941.4 eV which were incorporated in the shakeup feature. Consequently, it is deduced that the new feature at 932.6 eV was indicative of a Cu^{+} species due to the lack of an appropriate shakeup feature. This conclusion is supported by the investigation of Grünert *et al.* (21) which indicated that Cu_2O is characterized by a Cu $2p_{3/2}$ binding energy of 932.3 eV. Further, heating to 460°C (Fig. 6c) induced complete removal of the subbands originally at 944.9 and 936.7 eV, diminished the intensity of the subbands due to copper hydroxyl species, and enhanced the magnitude of the peak at 932.6 eV assigned to Cu^{+} species. Allowing the sample to equilibrate at 500°C (Fig. 6d) resulted in the appearance of a single peak at ca. 933.1 eV.

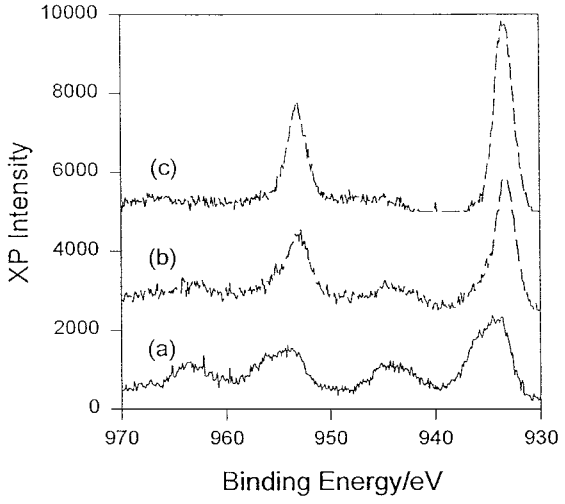

FIG. 7. *In situ* X-ray photoelectron spectra illustrating autoreduction of calcined Cu-ZSM-5-195 at (a) 20, (b) 200, and (c) 500°C.

Autoreduction. A calcined Cu-ZSM-5-195 sample was mounted on the heated probe and *in situ* XPS spectra were recorded during heating of the catalyst to 500°C *in vacuo* (Fig. 7). As the catalyst was heated to 200°C the intensity of the shakeup features was generally attenuated and simultaneously peaks at 953.2 and 933.8 eV developed. Grünert *et al.* (21) have identified similar trends when heating Cu-ZSM-5 catalysts under vacuum conditions. Further heating resulted in the complete disappearance of the satellite features which suggested the complete conversion of Cu^{2+} species to Cu^{+} moieties. However, although short acquisition times were used to record these *in situ* XPS spectra we have severe reservations about their accuracy. There is significant evidence of the formation of Cu^{+} species during autoreduction conditions (14, 16) but it is highly probable that the X-ray flux induces the reduction of copper oxide species at elevated temperature. This matter is discussed below.

Temperature-Programmed Decomposition

To further probe the nature of the changes induced by heating the precursor species a sample of Cu-ZSM-5-195 was placed in the microreactor and linearly heated to 600°C while the evolved gases were continuous monitored by on-line mass spectrometry. The resultant temperature-programmed decomposition profile is displayed in Fig. 8. The major species to be lost was water which evolved between 30 and 473°C. Deconvolution of the water profile (Fig. 8) indicated that at least seven distinct process were occurring with maximum rates of desorption at ca. 41, 122, 174, 239, 275, 384, and 563°C. The first two losses of water at 41 and 122°C probably correlated with the loss of physisorbed water from the zeolite structure. The loss of water at 174°C is consistent with the evolution of water molecules that are complexed to transition metal sites. The next feature at 239°C may be associated with the removal of water molecules complexed more strongly to copper sites on the zeolite surface. Kuroda *et al.* (25) reported a water loss from copper-exchanged mordenite at 350°C that was attributed to the loss of bridging hydroxyl species from a polynuclear copper species of general formula $[Cu_x(OH)_y]^{(2x-y)+}$, and we propose a similar assignment for the water loss at 275°C. Simliarly, Schoonheydt *et al.* (26) found that water was produced at ca. 400°C from both metal-exchanged X and Y zeolites which was ascribed to the dehydroxylation of metal hydroxyl species. The temperature of this reported water desorption is consistent with the peak discerned in this study at 384°C. Finally, the highest-temperature water production at 563°C is similar to a value of ca. 600°C reported by Anpo *et al.* (27) for the removal of OH groups from a Cu-ZSM-5 surface.

Thermogravimetric Analysis

Complementary thermogravimetric studies were performed to examine the decomposition process on each Cu-ZSM-5 sample (Fig. 9). In each instance the DTG trace was dominated by a loss between ambient temperature and ca. 180°C which presumably was associated with the loss of physisorbed water from the zeolite pores. Using the sample with highest copper loading, Cu-ZSM-5-195, as an example showed definite losses at 245, 295, 390, and 500°C (Fig. 9). The positions of these peaks correlated well with those subbands calculated in the temperature-programmed desorption profile (Fig. 8). Consequently, the same assignments are proposed as outlined above.

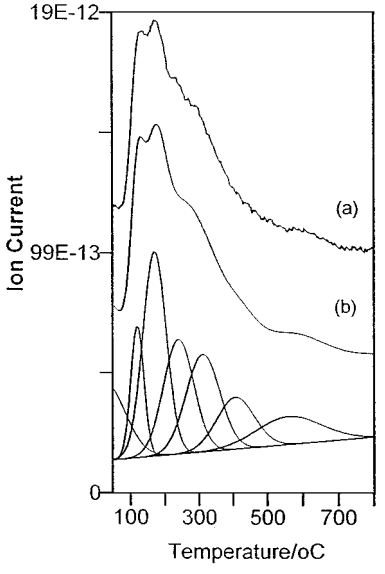

FIG. 8. Temperature-programmed decomposition of uncalcined Cu-ZSM-5-195: (a) $m/e = 18$, (b) resultant fit, (c) calculated subbands.

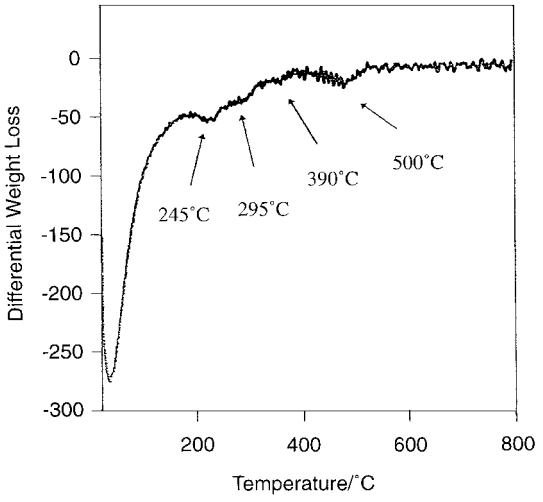

FIG. 9. TGA trace recorded for the decomposition of precursor species on Cu-ZSM-5-195.

Temperature-Programmed Desorption of Oxygen

Each Cu-ZSM-5 sample was calcined *in situ* in oxygen at 500°C and then cooled in oxygen to ambient temperature whereupon the catalyst was flushed in helium. Subsequently, the Cu-ZSM-5 was linearly heated at 20°C/min and the gaseous species produced were continuously monitored by on-line mass spectrometry. The collected TPD profiles are shown in Fig. 10. No desorption of oxygen was noted for either the under-exchanged Cu-ZSM-5 sample (Fig. 10a) or the catalyst exchanged at pH 5.5 (Fig. 10b). However, two main features were determined with T_{max} values of 407 and 575°C for the Cu-ZSM-5-6.0 catalyst (Fig. 10c) and these were substantially enhanced in magnitude for the highest copper-exchanged ZSM-5 sample (Fig. 10d). In addition, a minor desorption at ca. 111°C was also discerned in Figs. 10c and 10d. Valyon and Hall (13) have reported similar oxygen desorption phenomena at 125, 218, 410, and 550°C for a 114% copper-exchanged ZSM-5 catalyst, the lowest-temperature desorption being attributed to molecularly bound species and the higher-temperature processes to removal of extra-lattice oxygen species. Curve-fitting procedures were applied to the profile shown in Fig. 10d and the ratio of the area of the subband at 575°C relative to that at 407°C was calculated to be 1.8.

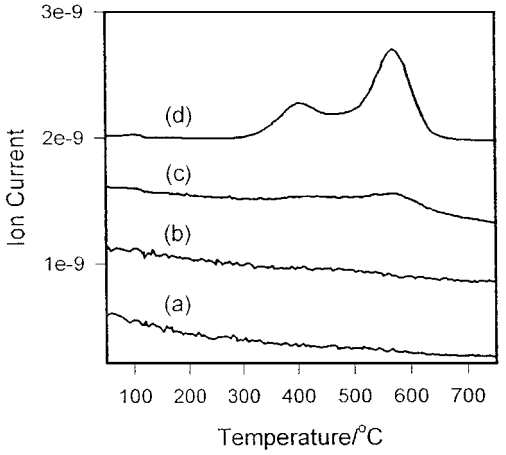

FIG. 10. Temperature-programmed desorption of oxygen ($m/e = 32$) from calcined (a) Cu-ZSM-5-52, (b) Cu-ZSM-5-54, (c) Cu-ZSM-5-102, and (d) Cu-ZSM-5-195.

FTIR Spectroscopy

Carbon Monoxide Adsorption

Influence of CO partial pressure. The effect of the carbon monoxide partial pressure on the nature of the adsorbates formed was investigated by varying the CO concentration from 0.1 to 1%. Figure 11 displays the spectra obtained following exposure of carbon monoxide to the Cu-ZSM-5-195-CO sample. Initially a band at 2155 cm^{-1} was discerned (Fig. 11a) which was in excellent agreement with the data of Spoto *et al.* (28) and Aylor *et al.* (17) for the ν(CO) mode of a linearly adsorbed CO species on a Cu^+ site. As the partial pressure of CO was increased (Figs. 11b–11f) bands developed at 2176 and 2149 cm^{-1} that were typical for the symmetric and asymmetric stretching vibrations of a *gem*-dicarbonyl species [$Cu^+(CO)_2$] (28).

Flushing the sample with helium at ambient temperature not unexpectedly resulted in the rapid removal of bands due to gaseous carbon monoxide and also induced the disappearance of the peaks characteristic of the *gem*-dicarbonyl species (Fig. 12a). An intense band at 2157 cm^{-1} due to the presence of Cu^+–CO remained and a shoulder at ca. 2143 cm^{-1} was also apparent. To more precisely identify

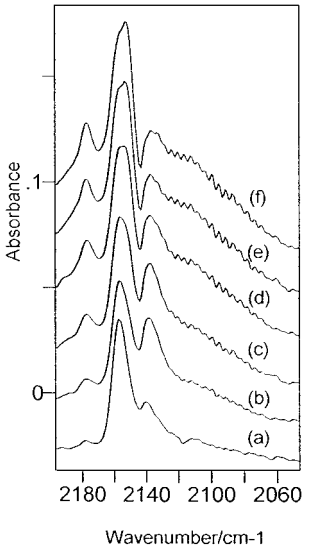

FIG. 11. *In situ* FTIR spectra of the exposure of CO to a CO-reduced Cu-ZSM-5-195 sample at 20°C and pressures of (a) 0.1, (b) 0.3, (c) 0.5, (d) 0.7, (e) 0.9, and (f) 1% CO in He.

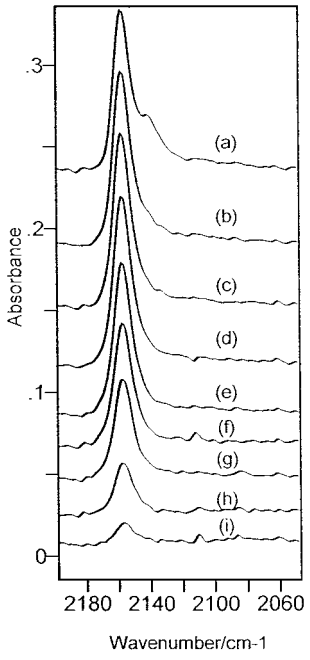

FIG. 12. (a) Spectrum of Cu-ZSM-5-195 after exposure to 1% CO followed by flushing with helium at 293 K. FTIR spectra obtained during heating of sample at 20°C/min: (b) 90, (c) 120, (d) 150, (e) 210, (f) 270, (g) 300, (h) 360, and (i) 420°C.

the adsorbed CO species, curve-fitting procedures were employed to deconvolute this profile (Fig. 13). Three subbands were calculated at 2157, 2143, and 2117 cm^{-1} with FWHM values of 12, 24, and 32 cm^{-1}, respectively. The adsorption of CO on Cu_2O gives rise to an IR band at 2125 to 2115 cm^{-1} (depending on the precise morphology of the Cu_2O) (29). Consequently, it is reasonable to assign the peak at 2117 cm^{-1} to a vibration for linear CO adsorbed on Cu_2O. The position of the vibrational mode at 2143 cm^{-1} is similar to a band reported by Lokhov *et al.* (30) at 2148 cm^{-1} ascribed to CO adsorption on an anionic vacancy on CuO. This assignment is plausible as the pretreatment procedure employed in this study is sufficient only to partially reduce CuO species that are present (cf. Fig. 10).

Heating the CO-exposed Cu-ZSM-5-195-CO sample resulted in the rapid disappearance of the species characterized by bands at 2143 and 2117 cm^{-1} (Figs. 12b–12d). In contrast, the species represented by a peak at 2157 cm^{-1} was exceptionally stable and did not fully desorb until a temperature in excess of 420°C.

Influence of copper loading. As already indicated the extent of copper exchange on the zeolite surface has a critical effect on the catalytic activity of these catalysts, especially with respect to the direct decomposition of NO (29). Therefore, the series of copper-exchanged catalysts of interest in this study were all exposed to a 1% mixture of CO/He for 10 min and then flushed with helium for 10 min. Subsequently, infrared spectra were accumulated and the resultant data are displayed in Fig. 14. As a general observation, all samples exhibited a peak at 2157 cm^{-1} due to the presence of Cu^+–CO species although it was apparent that the intensity of this mode was dependent on the concentration of copper present. The formation of species responsible for the shoulder at ca. 2143 cm^{-1} was promoted at higher copper exchange levels, and these data and the latter results are summarized in Table 2 to aid interpretation.

Importance of the reduction procedure. Aylor *et al.* (17) have compared the influence of autoreduction versus CO

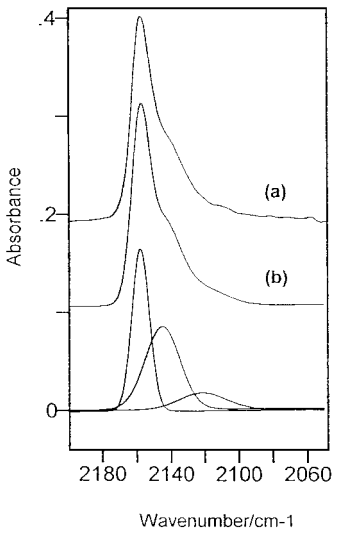

FIG. 13. FTIR spectrum of (a) CO adsorption on Cu-ZSM-5-195 after flushing in helium at ambient temperature. (b) Curve-fit profile. Remaining features are the calculated subbands.

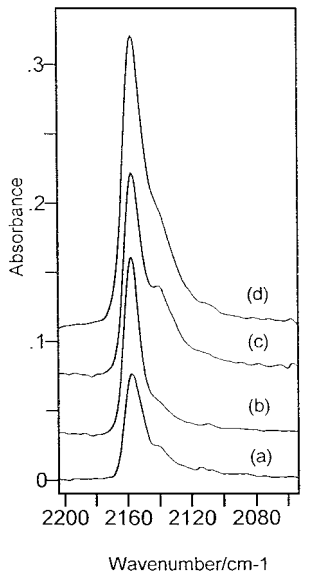

FIG. 14. FTIR spectra obtained after exposure of 1% CO and subsequent flushing in helium at 293 K of (a) Cu-ZSM-5-52, (b) Cu-ZSM-5-54, (c) Cu-ZSM-5-102, and (d) Cu-ZSM-5-195.

TABLE 2

Comparison of the Intensities of Various FTIR Subbands Identified after CO Adsorption on Under- and Overexchanged Reduced Cu-ZSM-5 Catalysts

	2157 cm^{-1}	2143 cm^{-1}	2117 cm^{-1}
Cu-ZSM-5-195	2.12	2.16	0.58
Cu-ZSM-5-102	1.37	1.57	0.42
Cu-ZSM-5- 54	1.46	0.85	0.24
Cu-ZSM-5-52	0.78	0.56	0.24

TABLE 3

Influence of Reduction Procedure on Intensity of Observed FTIR Subbands following CO Adsorption on Cu-ZSM-5-195 at Ambient Temperature

	2157 cm^{-1}	2143 cm^{-1}	2117 cm^{-1}
CO reduction	2.12	2.16	0.58
Auto reduction	1.9	1.72	0.36
H_2 reduction	0.61	0.54	0.19

reduction of a 98% exchanged Cu-ZSM-5 catalysts on the subsequent adsorption of carbon monoxide. This study further develops this previous investigation by examining the effects of autoreduction and hydrogen and carbon monoxide reduction on the infrared spectra of CO on overexchanged Cu-ZSM-5. Figure 15 shows that the CO adsorption profile was indeed dependent on the reduction procedure employed, and to illustrate the observed differences curve-fitting of the spectra was performed. The resultant data are summarized in Table 3. It can be concluded that the intensity of all three calculated subbands is enhanced by the use of CO as a reductant and conversely the use of hydrogen severely attenuated all of the subbands (relative to the autoreduction procedure) (Fig. 15). Jang *et al.* (11) have reported that the intensity of bands due to adsorbed CO was greater after using CO reduction (relative to autoreduction). In contrast, Aylor *et al.* (17) have observed that the intensities of the bands for chemisorbed CO for autoreduced and CO reduced Cu-ZSM-5 samples were similar although they also noted that the intensity of the adsorbate peaks was dependent on the interaction time of CO with the catalyst. Concomitantly, the evolution of carbon dioxide was recorded and thus a surface reduction process must have occurred.

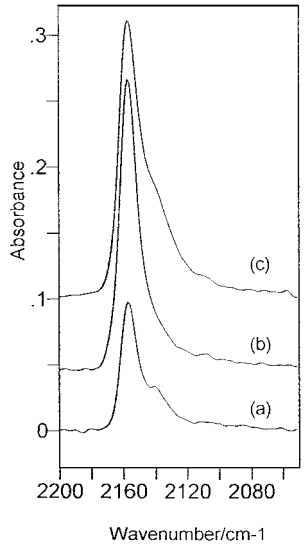

FIG. 15. Effect of different reduction conditions on CO adsorption FTIR spectra on Cu-ZSM-5-195: (a) hydrogen reduced, (b) autoreduced, (c) carbon monoxide reduced.

Sarkany *et al.* (14) used TPR methods on oxidized Cu-ZSM-5 to infer that hydrogen was a stronger reductant than CO, and postulated that hydrogen could reduce Cu^{2+} ions to Cu^+ species (>170°C), Cu^+ ions to Cu^0 (335°C) copper species containing extra-lattice oxygen (20°C), and CuO to copper metal (170°C). Consequently, it can be concluded that the conditions used in this study were sufficient to reduce a significant fraction of the oxidized copper species to copper metal. CO is known to be adsorbed exceptionally strongly on Cu^+ sites on the zeolite lattice but only weakly on Cu^{2+} and Cu^0 sites (29), thus explaining the decrease in CO band intensity when hydrogen is used as a reductant.

DISCUSSION

Nature of Precursor Species

XPS suggests the presence of at least three distinct copper environments on ZSM-5 following ion-exchange treatment with aqueous copper(II) acetate. The EPR studies of Giamello *et al.* (31) have indicated that three EPR active Cu^{2+} sites were present although no specific assignment was provided. The species represented by an XPS peak at ca. 933.7 eV was prevalent on the low copper-exchanged samples and appeared to be relatively stable to heat treatment to temperatures up to 450°C (Fig. 6). Kucherov *et al.* (32) also reported that the copper species incorporated into low copper-exchanged ZSM-5 catalysts do not reduce to Cu(I) species after heating in helium to 500°C. Parillo *et al.* (33) discovered that copper species exchanged with Brønsted acid sites on H-ZSM-5 in a 1 : 1 ratio and thus inferred that $[CuOH]^+$ species were present in solution. However, Lei *et al.* (15) have suggested that $[Cu_2(OH)_2]^{2+}$ species dominate if the solution pH is near neutral and this has resulted in Kharas *et al.* (5) postulating the reaction

$$ZO_2H^+ + [Cu_2(OH)_2]^{2+}(aq) \Rightarrow ZO_2Cu^{2+}OH^- + [Cu(OH_2)]^{2+}(aq),$$

where Z = Si and Al atoms of the zeolite lattice.

The position of the subband at 933.7 eV is consistent with a species with a net charge of 1+ (such as $ZO_2Cu^{2+}OH^-$) and with copper in an oxidation state of II. Furthermore, the intensity of the corresponding satellite feature for this species was comparatively low ($I_s/I_p = 0.12$–0.21). Okamoto *et al.* (34) reported that shakeup features become less intense as the coordination changes from octahedral to tetrahedral geometry. Thus we propose that the CuOH sites on ZSM-5 probably have a water molecule ligated to the complex as it is predicted that copper ions containing an ELO species are bonded to two oxygen ions in the zeolite lattice (35). Therefore, the additional water molecule would allow tetrahedral symmetry to be obtained:

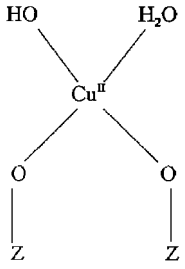

Species I

From the temperature-programmed desorption data regarding water evolution during autodecomposition of fresh Cu-ZSM-5 (Fig. 8) it is proposed that the feature with maximum rate of desorption at 174°C is due (at least in part) to the desorption of the water molecule bound to the copper(II) site in Species I. Consistent with this interpretation is the water loss at 550°C which was approximately half the intensity of the peak at 174°C. This latter observation is in harmony with the reaction that was previously postulated by Larsen and co-workers (17) for autoreduction of Cu^{2+} to Cu^+,

$$2[Cu^{2+}OH^-]^+ \Rightarrow Cu^+ + Cu^{2+}O^- + H_2O,$$

since one water molecule is produced by interaction of hydroxyl species from two copper sites. In contrast, the lower-temperature water desorption of ligated water at 174°C allows one molecule to be released from each copper site. Therefore, the ratio for the quantity of H_2O desorbed at low temperature compared with the amount desorbed due to recombinative desorption of hydroxyl species should theoretically be 2. This latter value is remarkably similar to the observed ratio of 1.98 recorded in this study.

Lei *et al.* (15) deduced that ESR-silent $[Cu_2(\mu\text{-}OH)_2]^{2+}$ species were present at higher copper loadings although there is insufficient evidence as yet to definitely prove the existence of this latter species. The XPS data do indicate the presence of a species with binding energy values close to those for $Cu(OH)_2$ especially as the zeolite sample becomes overexchanged with copper (Fig. 2D). It may be that very small clusters of $Cu(OH)_2$ may have been formed on the catalyst surface; however, the idea of Kharas *et al.* (5) that the reaction

$$ZO_2CuOH(OH_2) + [Cu_2(OH)_2]^{2+}(aq) \Rightarrow ZO_2Cu(OH)_2CuOH + [Cu(OH)_2]^{2+}$$

may have occurred cannot be discounted (or indeed could the proposal that higher oligomers could form). However, it is of relevance to consider the data of Kasusaka and co-workers (36–39) regarding the formation of novel binuclear copper oxide catalysts from cupric acetate monohydrate. The impregnation of silica by the acetate complex resulted in the formation of a highly dispersed binuclear structure comparable to that found in the parent copper(II) acetate monohydrate. On calcination this surface species was converted to chains of CuO parallelogram units which exhibited exceptional catalytic activity for the oxidation of CO by N_2O (37).

From the TGA and TPD study (peaks at 275 and 384°C) it appears that a combination of $Cu(OH)_2$ species and oligomeric hydroxycopper species suggested by Kharas *et al.* (5) may have formed (designated Species II).

Finally, the third copper species identified by XPS was located at a relatively high binding energy and therefore is evidently more ionic in character than the other two species characterized (20, 21). Haack and Shelef (20) assigned the copper species giving rise to a peak at ca. 936 eV to Cu^{2+} ions incorporated into the zeolite lattice. We propose that these species are possibly coordinated to four lattice oxygen ions with two water molecules ligated to this copper site to provide overall octahedral symmetry. XPS has shown that this species is characterized by a core line at 936.8 eV and a satellite at 944.8 eV. The intensity ratio of the satellite to the main peak (I_s/I_p) ranges from 0.46 to 0.58 which is consistent with the analysis of Okamoto *et al.* (34) for Cu^{2+} ions in octahedral coordination. Furthermore, EPR measurements of Larsen *et al.* (17), Lei *et al.* (15) and Anderson and Keran (40) have revealed the presence of octahedral copper complexes in hydrated Cu-ZSM-5 samples. $Cu(OH)_2$ and $Cu(H_2O)_6^{2+}$ may have been some of the octahedral species detected by EPR; however, XPS does indicate a copper species bound to the zeolite lattice in an octahedral structure as well and thus we propose that the following species may exist:

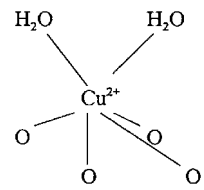

Species III

The precise orientation of Cu^{2+} with respect to the oxygen ions of the zeolite lattice cannot be ascertained from this study; the copper species may be in the same plane as the oxygen ions or alternatively it may be above the oxygen plane (as shown in the diagram). Another problem to ponder is the identification of the sites where these copper species are located. The theoretical study of Trout *et al.* (35) may reveal more information on this topic. These authors have evaluated the possibility of locating a Cu^{2+} ion in a site that contains two Al-substituted T sites. It was deduced that placement of Cu^{2+} in the center of a six-membered ring was energetically unfavorable due to excessively long Cu–O bond lengths. In contrast, inclusion of Cu^{2+} in a five-membered ring resulted in Cu–O bond distances that were more acceptable and it was indicated that at least four bonds to oxygen sites adjacent to aluminum sites were possible.

Transformations during Autodecomposition

The decomposition of the precursor species during heating *in vacuo* or helium at high temperature should result in the following changes to the copper sites present following the exchange procedure:

Species I

$$ZO_2[Cu^{2+}OH^-]^+ \cdot H_2O \Rightarrow ZO_2[Cu^{2+}OH^-]^+ + H_2O \quad 239^\circ C \quad (1)$$

$$2ZO_2[Cu^{2+}OH^-]^+ \Rightarrow ZO_2Cu^+ + ZO_2Cu^{2+}O^- + H_2O \quad 550^\circ C \quad (2)$$

Species II

$$ZO_2Cu(OH)_2CuOH \Rightarrow ZO_2CuOCuOH + H_2O \quad 275^\circ C \quad (3)$$

$$Cu(OH)_2 \Rightarrow CuO + H_2O \quad 384^\circ C \quad (4)$$

Species III

$$ZO_4Cu^{II}(H_2O)_2 \Rightarrow ZO_4Cu^{II} + 2\,H_2O \quad 174^\circ C \quad (5)$$

Consequently, from the mass spectrum recorded in Fig. 8 it should be possible to calculate the relative concentrations of the copper species present. A summary of these data is provided in Table 4, and for comparison the concentrations of the three copper species in sample Cu-ZSM-5-195 as obtained by XPS at ambient temperature are shown. XPS studies indicated (Fig. 6) that heating the precursor sample to 200°C was sufficient to initiate the conversion of Cu(II) ions characterized by a peak at ca. 936.8 eV to Cu(I) ions. However, we strongly feel that this effect was an artifact caused by sample degradation due to the X-ray flux. Thus, we include the *in situ* XPS spectra as a warning to other researchers of the difficulties in obtaining XPS spectra of copper zeolites. We emphasize that spectra should be acquired either using short acquisition times at ambient temperature or, alternatively, at subambient temperatures.

TABLE 4

Concentrations of Cu Species Found in Cu-ZSM-5-195 by XPS and Mass Spectrometry of Desorption Products[a]

	Species I	Species II	Species III
XPS	31	47	22
Mass spectrometry	27	43.5	29.5

[a] Species I: Cu^{2+} ions coordinated to two-lattice-oxygen species. Species II small CuO clusters and Species III: Cu^{2+} ions coordinated to a four-lattice-oxygen species.

The TPD studies of the calcined samples indicate that autoreduction of Cu-ZSM-5-195 at temperatures between 500 and 550°C should be sufficient to reduce the "CuO" species to "Cu_2O" and the $ZO_2Cu^{2+}O_2^-$ species to ZO_2Cu^+ structures. The Cu^{2+} sites bound to four lattice oxygen ions are thought to be stable to autoreduction. Consequently, from Table 4 it can be deduced that between 71 and 78% of the Cu^{2+} ions originally present in Cu-ZSM-5 can be reduced to Cu^+ species by autoreduction. Liu and Robota (9) used *in situ* XANES to determine that autoreduction of Cu-ZSM-5 in helium at 550°C reduced 70% of Cu(II) species to Cu(I) which is in excellent agreement with our data.

Also relevant is the correlation between our XPS/TPD study and previous EPR investigations. The $ZO_2Cu^{2+}O^-$ species has been shown to be EPR silent (35) and naturally ZO_2Cu^+ species will not be EPR active. The Cu^{2+} ions coordinated to four oxygen ions in the zeolite lattice (ZO_4Cu^{2+}) will be EPR detectable and these species represent approximately 29 and 35% of the copper ions in Cu-ZSM-5-195 and Cu-ZSM-5-102, respectively. The copper oxide species present will be in the I oxidation state following autoreduction and thus will not be EPR active. Larsen *et al.* (17) used EPR to conclude that 40–60% of Cu^{2+} species are reduced to Cu^+ species during autoreduction conditions. Close inspection of these data reveals that as the copper-exchange level is elevated the quantity of Cu^{2+} species observed by EPR after autoreduction diminishes. Indeed, at an exchange level of 110% Cu only 40% of the copper ions are detected after autoreduction. This value is in reasonable agreement with our calculations which suggest that 29–35% of the copper ions should be observable. Extension of the data provided by Larsen *et al.* (17) to even higher copper-exchange levels that correlate better to this study would result in an even closer correspondence between the XPS/TPD data and EPR investigation. The *in situ* XANES study of Liu and Robota (9) supports this argument since a Cu-ZSM-5 catalyst exchanged to a copper level of 164% transformed into a sample containing 30% Cu(II) and 70% Cu(I) species following autoreduction.

Copper Sites Identified by CO Adsorption

Each Cu-ZSM-5 sample consisted of Cu^+ sites following reduction that adsorbed CO to form a complex with a characteristic vibrational frequency of 2157 cm^{-1}. In the presence of relatively large partial pressures of CO this latter species transformed into a *gem*-dicarbonyl moiety represented by infrared bands at 2149 and 2176 cm^{-1}. Subsequent reduction of the CO pressure resulted in the reformation of the linear adsorbed CO species. An unusual aspect of the adsorbed CO species on Cu^+ ions in the zeolite lattice was the remarkable thermal stability observed. Chemisorbed CO did not desorb at a maximum rate until a temperature of ca. 300°C. These data may indicate that the Cu^+ site is coordinated to the zeolite lattice in a unique manner. From the XPS studies it was concluded that copper sites existed in the zeolite lattice where Cu ions were bound to either two or four oxygen ions, respectively. It would thus appear that the strongly bound CO is associated with the copper ions coordinated to only two lattice oxygen species.

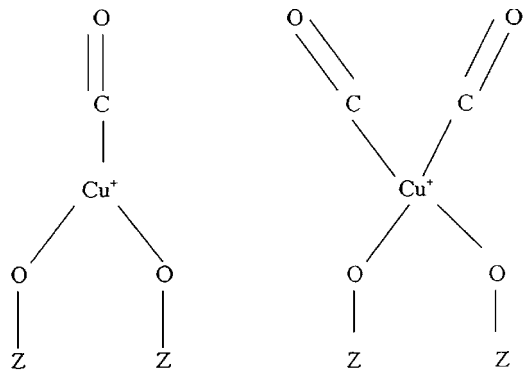

2157 cm^{-1} 2149 and 2176 cm^{-1}

It was also apparent that CO could reduce oxidic species that were stable to heating in an inert atmosphere. Equation [2] has shown that $ZO_2Cu^{2+}O^-$ species are produced during autodecomposition conditions. The theoretical predictions of Trout *et al.* (35) indicate that it is very unlikely that desorption of a single extra-lattice-oxygen atom will occur. However, Sachtler and co-workers (14, 15) have shown that ELO species can be readily removed in the presence of a suitable reductant. Consequently; CO can reduce these latter sites to Cu^+ species by the following mechanism:

$$ZO_2Cu^{2+}O^- + CO \Rightarrow ZO_2Cu^+ + CO_2,$$
$$ZO_2Cu^+ + CO \Rightarrow ZO_2Cu^+CO.$$

Thus, it is concluded that CO reduction should result in an increase in the number of Cu^+ species that can be detected by infrared spectroscopy (relative to autoreduction). Nevertheless, whether this effect is detected or not is highly dependent on the exact experimental conditions employed since the adsorption of CO on an autoreduced sample during infrared measurements will be sufficient to initiate further sample reduction. Hadjiivanov *et al.* (41) have also noted the fact that room-temperature exposure of CO during FTIR investigations can result in catalyst reduction. The observation of Cu^+ species in oxidized Cu-ZSM-5 using CO as an infrared probe molecule by Jang *et al.* (11) was probably a consequence of the aforementioned reduction of ELO species by the adsorbed CO.

Several authors have discussed the possibility of copper oxide formation in Cu-ZSM- 5 catalysts (8, 20). FTIR spectroscopy of CO adsorption (Fig. 13) has indicated that CuO species are present on the surface of the zeolite (band 2143 cm^{-1}). These data are in accordance with the results of the XPS study (see above).

We have shown here through XPS that three possible species of copper probably exist in the framework of ZSM-5, in particular a low-coordinated species of copper, which is believed to be the active species directly involved in NO decomposition. It has been demonstrated by Attfield *et al.* (42, 43) that the structure of ZSM-5, or in fact the pentasil zeolite family in general, is important in producing a low-coordinated extra-framework Cu^{2+} cation in the dehydrated copper ion zeolite. It is possible that the more accessible the active Cu^{2+} ion is to the incoming NO molecule, the greater chance the zeolite has of being an active catalyst. Attfield *et al.* showed that for Cu-ferrierite the Cu^{2+} ions are poorly coordinated to the zeolite framework and are highly accessible to reacting molecules passing through the channel. Significantly, they are not situated within the sodalite cage of the zeolite where reactant molecules cannot reach. In contrast, copper-exchanged X and Y zeolites are inactive as deNO_x catalysts as the Cu^{2+} species are found highly coordinated in the sodalite cage and are inaccessible to the incoming reactant molecules.

CONCLUSIONS

1. Several distinct copper species exist in Cu-ZSM-5 catalysts: (i) Cu^{2+} ions coordinated to a four-lattice-oxygen species, (ii) Cu^{2+} ions coordinated to two-lattice-oxygen species, and (iii) small CuO clusters.
2. Extra-lattice-oxygen species were bound to the Cu^{2+} ions coordinated to two-lattice-oxygen species.
3. Autoreduction of Cu^{2+} ions coordinated to two-lattice-oxygen species created Cu^+ species that could strongly bind adsorbed CO.
4. The unique activity of Cu-ZSM-5 catalysts for NO reduction is probably associated with the presence of Cu^{2+} ions coordinated to only two-lattice-oxygen species.

REFERENCES

1. Taylor, K. C., *Catal. Rev. Sci. Eng.* **35**, 457 (1993).
2. Shelef, M., *Chem. Rev.* **95**, 209 (1995).

3. Armor, J. N., *Catal. Today* **26**, 147 (1995).
4. Walker, A. P., *Catal. Today* **26**, 107 (1995).
5. Kharas, K. C., Liu, D-J., and Robota, H. J., *Catal. Today* **26**, 129 (1995).
6. Iwamoto, M., Yahiro, H., Mine, Y., and Kagawa, S., *Chem. Lett.*, 213 (1989).
7. Grinsted, R. A., Jen, H-W., Montreuil, C. N., Rokosz, M. J., and Shelef, M., *Zeolites* **13**, 602 (1993).
8. Centi, G., and Perathoner, S., *Appl. Catal. A* **132**, 179 (1995).
9. Liu, D-J., and Robota, H. J., *Catal. Lett.* **21**, 291 (1993).
10. Liu, D-J., and Robota, H. J., *Appl. Catal. B* **4**, 155 (1994).
11. Jang, H-J., Hall, W. K., and d'Itri, J., *J. Phys. Chem.* **100**, 9416 (1996).
12. Valyon, J., and Hall, W. K., *J. Phys. Chem.* **97**, 7054 (1993).
13. Valyon, J., and Hall, W. K., *J. Catal.* **143**, 520 (1993).
14. Sarkany, J., d'Itri, J. L., and Sachtler, W. M. H., *Catal. Lett.* **16**, 241 (1992).
15. Lei, G. D., Adelman, B. J., Sarkany, J., and Sachtler, W. M. H., *Appl. Catal. B* **5**, 245 (1995).
16. Larsen, S. C., Aylor, A. W., Bell, A. T., and Reimer, J. A., *J. Phys. Chem.* **98**, 11533 (1994).
17. Aylor, A. W., Larsen, S. C., Reimer, J. A., and Bell, A. T., *J. Catal.* **157**, 592 (1995).
18. Chang, Y-F., and McCarty, J. G., *J. Catal.* **165**, 1 (1997).
19. Zhang, Y., Leo, K. M., Sarofim, A. F., Hu, Z., and Flytzani-Stephanopoulos, M., *Catal. Lett.* **31**, 75 (1995).
20. Haack, L. P., and Shelef, M., *in* "Proceedings of the Symposium on Catalytic Reduction of NO_x, ACS Spring Meeting, Denver, March 1993."
21. Grunert, W., Hayes, N. W., Joyner, R. W., Shapiro, E. S., Rafiq, M., Siddiqui, H., and Baeva, G. N., *J. Phys. Chem.* **98**, 10832 (1994).
22. Basu, P., Ballinger, T. H., and Yates, J. T., *Rev. Sci. Instrum.* **59**, 1321 (1998).
23. Wagner, C. D., Riggs, W. M., Davis, L. E., and Moulder, J. F., *in* "The Handbook of X-ray Photoelectron Spectroscopy" (G. E. Muilenberg, Ed.), p. 82. Perkin–Elmer Corp. 1979.
24. Frost, J. C., *Nature* **334**, 577 (1988).
25. Kuroda, Y., Kotani, A., Maeda, H., Moriwaki, H., Morimato, T., and Nagao, M., *J. Chem. Soc. Faraday Trans.* **88**, 1583 (1992).
26. Schoonheydt, R. A., Vandamme, L. J., Jacobs, P. A., and Uytterhoeven, J. B., *J. Catal.* **43**, 292 (1976).
27. Anpo, M., Matsuoka, M., Shioya, Y., Yamashita, H., Giamello, E., Morterra, C., Che, M., Patterson, H. H., Webber, S., Ouellette, S., and Fox, M. A., *J. Phys. Chem.* **98**, 5744 (1994).
28. Spoto, G., Zecchina, A., Bordiga, S., Ricchiardi, G., Martra, G., Loefanti, G., and Petrini, G., *Appl. Catal. B* **3**, 151 (1994).
29. Centi, G., Nigro, C., and Perathoner, S., *React. Kinet. Catal. Lett.* **53**, 79 (1994).
30. Lokhov, Yu. A., Sadykov, V. A., Tikhov, S. F., and Popouskii, V. V., *Kinet. Katal.* **26**, 152 (1985).
31. Giamello, E., Murphy, D., Magnacca, G., Morterra, C., Shioya, Y., Nomura, T., and Anpo, M., *J. Catal.* **136**, 510 (1992).
32. Kucherov, A. V., Gerlock, J. L., Jen, H-W., and Shelef, M., *J. Phys. Chem.* **98**, 4892 (1994).
33. Parillo, D. J., Dolenec, D., Gorte, R. J., and McCabe, R. W., *J. Catal.* **142**, 708 (1993).
34. Okamoto, Y., Fukino, K., Imanaka, T., and Teranishi, S., *J. Phys. Chem.* **87**, 3740 (1983).
35. Trout, B. L., Chakraborty, A. K., and Bell, A. T., *J. Phys. Chem.* **100**, 4173 (1996).
36. Nomura, M., Kazusaka, A., Kakuta, N., Ukisu, Y., and Miyahara, K., *J. Chem. Soc. Faraday Trans. 1* **83**, 1227 (1987).
37. Kakuta, N., Kazusaka, A., and Miyahara, K., *Bull. Chem. Soc. Japan* **59**, 3267 (1986).
38. Nomura, M., Kazusaka, A., Ukisu, Y., and Kakuta, N., *J. Chem. Soc. Faraday Trans. 1* **83**, 2635 (1987).
39. Kakuta, N., Kazusaka, A., Yamazaki, A., and Miyahara, K., *J. Chem. Soc. Faraday Trans. 1* **80**, 3245 (1984).
40. Anderson, M. W., and Kevan, L., *J. Phys. Chem.* **91**, 4174 (1987).
41. Hadjiivanov, K., Klissurski, D., Ramis, G., and Busca, G., *Appl. Catal. B* **7**, 251 (1996).
42. Attfield, M. P., Weigel, S. J., and Cheetham, A. K., *J.Catal.* **170**, 227 (1997).
43. Attfield, M. P., Weigel, S. J., and Cheetham, A. K., *J. Catal.* **172**, 274 (1997).